

**Abstract:** The structural stability, charge transfer effects and the strength of the spin-orbit couplings in different Ni(II)-ligand complexes with square-pyramidal and octahedral coordination have been studied at M06/def2-TZVP level of theory. Accordingly, two different, porphyrin- and diketo-pyrphyrin-based four-coordination macrocycles as planar ligands as well as pyridine, pyrrole and mesylate anion molecular groups as vertical ligands were considered in order to build the square-pyramidal and octahedral coordination configurations. For each molecular system the identification of equilibrium geometries and the intersystem crossing (ISC - the minimum energy crossing point) between the potential energy surfaces of the singlet and triplet spin states is followed by computing the spin-orbit couplings between the two spin states. Structures, based on the diketo-pyrphyrin macrocycle as planar ligand, show stronger five- and six-coordination organometallic complexes due to the extra electrostatic interaction between the positively charged central metal cation and the negatively charged vertical ligands. The results also show that the magnitude of the spin-orbit coupling is strongly influenced by the atomic positions of deprotonations of the ligands but not by the direction of the charge transfer between the ligand and the central metal ion.

## Method:

- The equilibrium geometries of the Ni(II)-ligand complexes with square-pyramidal and octahedral coordination have been obtained using the M06 [1] exchange-correlation functional (27% of HF-exchange) methods implemented in the Orca [2,3] program.
- The energy decomposition analysis have been made considering the pair natural orbital based local coupled cluster method (DLPNO-CCSD(T)) [4].

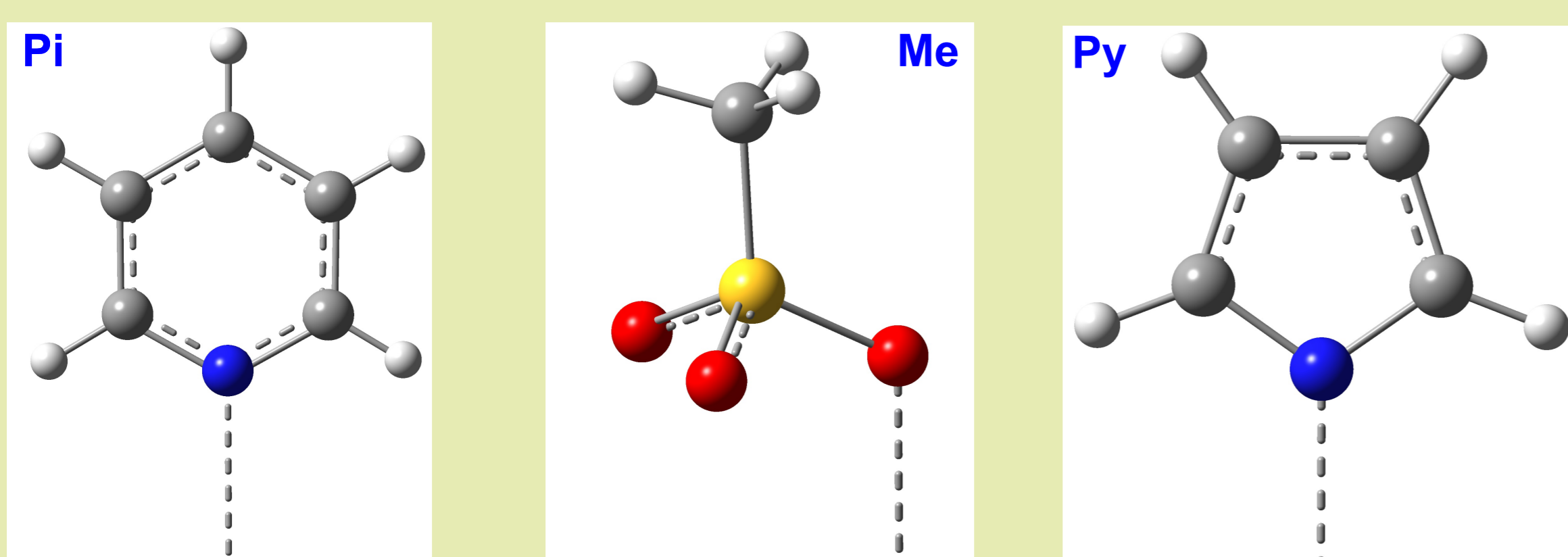


Figure 2. The vertical ligand fragments (Pi = pyridine; Me = mesylate; Py = Pyrrole) in the square-planar and octahedral Ni(II) macrocyclic ligand complexes.

Energy (kcal/mol)	P1Pi	P1Me	C1Py	C1Me
$\Delta E^S (X \leftrightarrow Y)$	-121.47	-154.74	-635.91	-426.12
$\Delta E^T (X \leftrightarrow Y)$	-164.74	-178.74	-681.95	-463.45
$\Delta CT^S (X \rightarrow Y)$	-1.27	-3.25	-1.33	-0.55
$\Delta CT^S (X \leftarrow Y)$	-10.23	-14.06	-36.55	-43.31
$\Delta CT^T (X \rightarrow Y)$	-1.33	-3.23	-1.35	-0.76
$\Delta CT^T (X \leftarrow Y)$	-11.76	-15.61	-38.73	-44.87
$\Delta Disp^S (X \leftrightarrow Y)$	-4.18	-4.91	-9.79	-5.68
$\Delta Disp^T (X \leftrightarrow Y)$	-4.23	-4.87	-9.63	-5.57

Figure 3. The total fragment interaction energies ( $\Delta E$ ) as well as their the charge transfer ( $\Delta CT$ ) and dispersion ( $\Delta Disp$ ) contributions. All values are given in kcal/mol.

Energy (kcal/mol)	P2Pi	P2Me	C2Py	C2Me
$\Delta E^S (X \leftrightarrow Y1)$	-87.67	-125.04	-228.21	-306.60
$\Delta E^S (X \leftrightarrow Y2)$	-87.89	-125.38	-228.59	-306.64
$\Delta E^T (X \leftrightarrow Y1)$	-107.29	-138.53	N/A	-311.99
$\Delta E^T (X \leftrightarrow Y2)$	-107.85	-138.74	N/A	-337.31
$\Delta CT^S (X \rightarrow Y1)$	-9.60	-14.40	-13.89	-33.10
$\Delta CT^S (X \rightarrow Y2)$	-9.61	-14.52	-14.00	-33.23
$\Delta CT^T (X \rightarrow Y1)$	-10.62	-15.77	N/A	-33.48
$\Delta CT^T (X \rightarrow Y2)$	-10.88	-15.82	N/A	-34.13

Figure 4. The total fragment interaction energies ( $\Delta E$ ) as well as their the charge transfer ( $\Delta CT$ ) and dispersion ( $\Delta Disp$ ) contributions. All values are given in kcal/mol.

## Acknowledgement:

This work was financially supported by CNCS-UEFISCDI (PN-III-P4-ID-PCE-2016-0208).

## References:

- Y. Zhao, D. Truhlar *Theoretical Chemistry Accounts*. 2008, 120, 215-241.
- F. Neese *Wiley Interdisciplinary Reviews-Computational Molecular Science*. 2012, 2, 73-78.
- F. Neese *Wiley Interdisciplinary Reviews-Computational Molecular Science*. 2018, 8, e1327.
- D. Liakos, A. Hansen, F. Neese *Journal of Chemical Theory and Computation*. 2011, 7, 76-87.

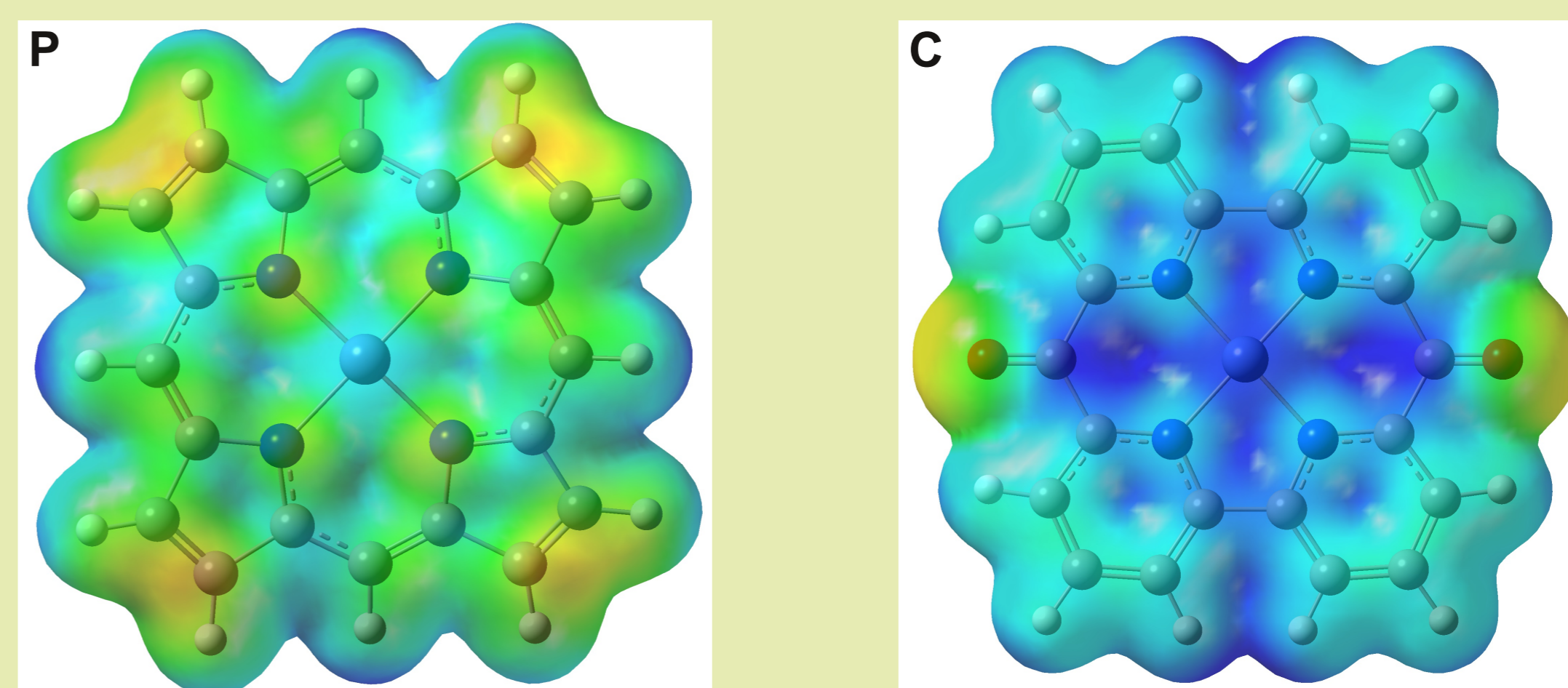


Figure 1. The two maps of the electrostatic potential ( $e_{min}=0.1e$  and  $e_{max}=0.3e$ ) for the Ni(II)<sup>2+</sup>-porphyrin<sup>2-</sup> (a) and of Ni(II)<sup>2+</sup>-diketo-pyrphyrin (b) complexes.

	Triplet Geom.	ISC Geom.	Singlet Geom.
<b>C2Me</b>			
Ni charge	T: 0.85e ( $\alpha$ : -0.35e; $\beta$ : 1.20e)	S: 0.62e T: 0.84e ( $\alpha$ : -0.34e; $\beta$ : 1.18e)	S: 0.69e
Ni el. conf.	T: 4s(0.23)3d(8.32)4p(0.56) $\alpha$ : 4s(0.11)3d(4.95)4p(0.27) $\beta$ : 4s(0.12)3d(3.37)4p(0.29)	S: 4s(0.24)3d(8.56)4p(0.56) T: 4s(0.24)3d(8.32)4p(0.58) $\alpha$ : 4s(0.12)3d(4.93)4p(0.28) $\beta$ : 4s(0.12)3d(3.39)4p(0.30)	S: 4s(0.25)3d(8.59)4p(0.45)
<b>P2Pi</b>			
Ni charge	T: 0.86e ( $\alpha$ : -0.34e; $\beta$ : 1.20e)	S: 0.65e T: 0.87e ( $\alpha$ : -0.33e; $\beta$ : 1.20e)	S: 0.75e
Ni el. conf.	T: 4s(0.23)3d(8.31)4p(0.57) $\alpha$ : 4s(0.11)3d(4.94)4p(0.27) $\beta$ : 4s(0.12)3d(3.37)4p(0.30)	S: 4s(0.23)3d(8.53)4p(0.57) T: 4s(0.22)3d(8.30)4p(0.59) $\alpha$ : 4s(0.11)3d(4.92)4p(0.29) $\beta$ : 4s(0.11)3d(3.38)4p(0.30)	S: 4s(0.25)3d(8.55)4p(0.44)

Figure 5. The natural charge distribution for the central Ni(II) atom in octahedral coordination configuration for the three characteristic geometries of the C2Me and P2Pi organometallic complexes.

SOC (cm <sup>-1</sup> )	P1Pi	P1Me	C1Py	C1Me
X	5.01	7.38	0.07	14.96
Y	6.39	2.59	0.53	6.27
Z	12.93	2.73	5.23	10.39
SOC (cm <sup>-1</sup> )	P2Pi	P2Me	C2Py	C2Me
X	0.37	4.45	8.62	4.96
Y	0.50	25.21	20.53	22.15
Z	3.87	0.52	9.01	3.48

Figure 6. The spin-orbit couplings (cm<sup>-1</sup>) along the X, Y and Z axes for the eight square-planar and octahedral Ni(II) macrocyclic ligand complexes.

## Conclusions:

- Based on the DLPNO-CCSD(T) energy decomposition analysis the diketo-pyrphyrin-based four-coordination macrocycles as planar ligands show better structural stability than those based on the porphyrin. The stability enhancement is given by the stronger bounding of the vertical ligands induced by the extra electrostatic interaction between the positively charged central Ni(II) ion and the negatively charged vertical ligands.
- The mesylate (CH<sub>3</sub>SO<sub>3</sub><sup>-</sup>) vertical ligand gives more stable square-planar or octahedral coordination configurations.
- Significant amount of charge redistribution during the singlet-triplet spin transition was found for the ISC geometries of C2Me and P2Pi complexes. At the same time, the triplet natural charge distributions of the equilibrium triplet and the ISC (or minimum energy crossing point) geometries are almost similar, indicating that the charge redistribution mainly occurs during the singlet-triplet spin transition.
- The mesylate (CH<sub>3</sub>SO<sub>3</sub><sup>-</sup>) vertical ligand gives stronger spin-orbit couplings, than those based on the pyridine and pyrrole, but they do not correlate with the Z axis (the direction of the charge transfer between the ligand and the central metal ion).